

# The identification of liquid ethane in Titan's Ontario Lacus

R. H. Brown<sup>1</sup>, L. A. Soderblom<sup>2</sup>, J. M. Soderblom<sup>1</sup>, R. N. Clark<sup>3</sup>, R. Jaumann<sup>4</sup>, J. W. Barnes<sup>5</sup>, C. Sotin<sup>6</sup>, B. Buratti<sup>6</sup>, K. H. Baines<sup>6</sup> & P. D. Nicholson<sup>7</sup>

Titan was once thought to have global oceans of light hydrocarbons on its surface<sup>1–5</sup>, but after 40 close flybys of Titan by the Cassini spacecraft, it has become clear that no such oceans exist<sup>6</sup>. There are, however, features similar to terrestrial lakes and seas<sup>7</sup>, and widespread evidence for fluvial erosion<sup>8,9</sup>, presumably driven by precipitation of liquid methane from Titan's dense, nitrogen-dominated atmosphere<sup>10</sup>. Here we report infrared spectroscopic data, obtained by the Visual and Infrared Mapping Spectrometer<sup>11</sup> (VIMS) on board the Cassini spacecraft, that strongly indicate that ethane, probably in liquid solution with methane, nitrogen and other low-molecular-mass hydrocarbons, is contained within Titan's Ontario Lacus.

Saturn's moon Titan has a thick atmosphere that makes studies of its surface difficult, except through specific atmospheric windows<sup>12,13</sup>, as a result of strong atmospheric absorptions and a ubiquitous haze<sup>10,14,15</sup>. Imaging spectroscopy is used to determine the chemical composition of the surfaces and atmospheres of planetary bodies<sup>16</sup>, and the VIMS<sup>11</sup> instrument on board the Cassini spacecraft is capable of such measurements. VIMS was used during Cassini's 38th close flyby of Titan (T38) to observe Ontario Lacus, a lake-like

feature in Titan's south-polar region found with the Cassini Imaging Science Subsystem (ISS) narrow-angle camera in mid-2005. During Cassini's T25 flyby, both VIMS and Cassini's radar instrument were used to observe a northern lake near 78° N, 250° W (ref. 17).

The spectral data obtained for the northern lake were too noisy for compositional analysis, but they indicate that it has an extremely low reflectance in the near-infrared (Fig. 1), consistent with that of Ontario Lacus. Further compositional studies of this lake and others in the north will have to wait until they are directly illuminated in northern spring during Cassini's extended missions.

In contrast, the observations of Ontario Lacus with VIMS were of much higher quality, and were obtained in favourable viewing geometry and at much higher spatial resolution. The 'shoreline' of Ontario Lacus (Fig. 1) is quite bright both in the visible and at 5  $\mu\text{m}$  relative to the much darker interior of the lake. There is also an annular area (hereafter referred to as the 'beach') just inside the shoreline that is intermediate in brightness and whose inner edge roughly follows the shape of Ontario's shoreline. The reflectivity of this region at 2 and 5  $\mu\text{m}$  is intermediate to that of the interior of Ontario Lacus and its shoreline.

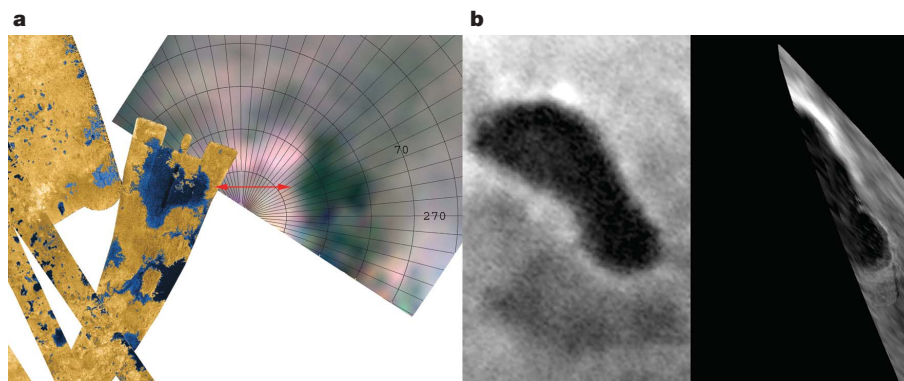


**Figure 1 | VIMS and radar images of the lake at 78° N, 250° W, and ISS and VIMS images of Ontario Lacus.** The red arrow indicates the same lake-like feature seen in radar (left side of **a**) and VIMS (right side of **a**). The VIMS image is congruent with the boundaries of the lake as seen in the radar image. The data were obtained at very large illumination angles (the lake was actually 5–10° past the terminator). VIMS observations of the northern lake were possible only because it was illuminated by light scattered past the terminator by Titan's atmosphere. Although the VIMS observations were far from ideal, the northern lake is well defined and is quite clearly the same lake as that imaged at much higher spatial resolution by the Cassini radar<sup>7</sup>. Note that the brightness distribution in the lake's interior as seen in the VIMS image roughly matches the intensity of the radar return as indicated in

shades of blue in the radar image. Colour in the VIMS image was constructed by assigning a band near 1.3  $\mu\text{m}$  to the blue channel, a band near 1.6  $\mu\text{m}$  to the green channel and a band near 2.0  $\mu\text{m}$  to the red channel. The ISS image (left side of **b**) from mid-2005 is compared with the VIMS image (right side of **b**). The VIMS image (taken during the T38 flyby, which occurred on 2007 December 4, at a closest approach altitude of 1,100 km, yielding a maximum resolution of about 500 m per pixel) is a co-addition of 11 channels in the 5- $\mu\text{m}$  window. The 'beach' is the thin annular area in the lower right of the image in **b**. It is intermediate in albedo between the lake interior and the surrounding shoreline, and is roughly congruent with the dark boundary of the lake interior and with the bright line delineating the shoreline.

<sup>1</sup>Department of Planetary Sciences, University of Arizona, Tucson, Arizona 85721, USA. <sup>2</sup>US Geological Survey, Flagstaff, Arizona 86001, USA. <sup>3</sup>US Geological Survey, Denver, Colorado 80225, USA. <sup>4</sup>Deutsches Zentrum für Luft- und Raumfahrt, 12489 Berlin, Germany. <sup>5</sup>NASA Ames Research Center, Moffett Field, California 94035, USA. <sup>6</sup>Jet Propulsion Laboratory, California Institute of Technology, Pasadena, California 91107, USA. <sup>7</sup>Department of Astronomy, Cornell University, Ithaca, New York 14853, USA.

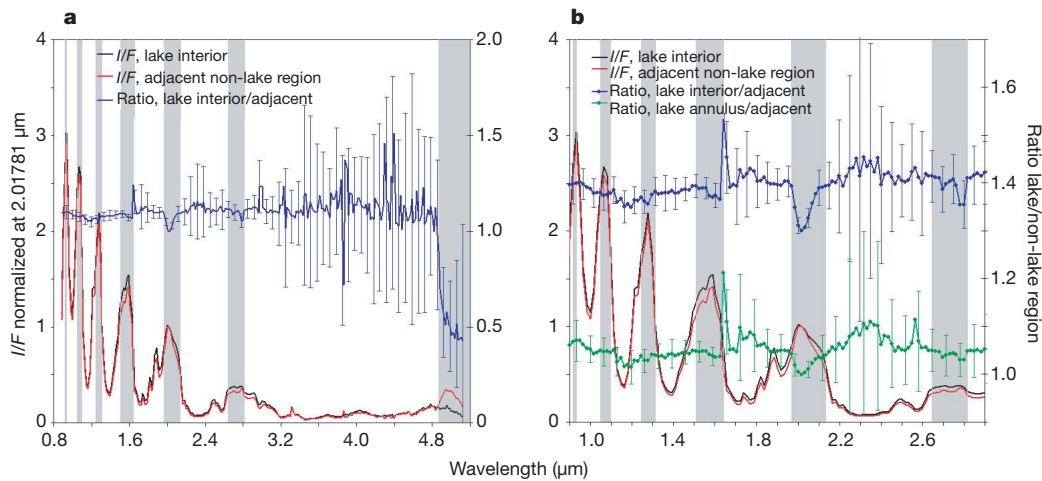


**Figure 2 | Spectra of regions in and around Ontario Lacus.** **a**, The  $I/F$  spectra ( $I$  is the observed specific intensity and  $\pi F$  is the incident solar flux) have been normalized to 1.0 at 2.0178  $\mu\text{m}$ , and the scale is on the left axis. The scale for the ratio spectrum is on the right axis. Even though the lake is intrinsically darker than its surroundings, the ratio is greater than 1.0 because of the normalization. This was done for clarity in the figures. **b**, A similar approach was used and a ratio spectrum for the ‘beach’ area is

included with a split right axis, again for the sake of clarity. Error bars have been shown for only every third point, again to improve clarity. The effectiveness of the atmospheric band removal is confirmed because the strong methane absorptions are nearly cancelled in the spectral ratio. The vertical grey bands in both panels denote the spectral channels within atmospheric windows through which VIMS can resolve surface detail. Error bars are  $1\sigma$ .

Titan’s atmospheric windows at 2.0, 2.7 and 5.0  $\mu\text{m}$  are amenable to surface composition studies<sup>13,18–20</sup>, and within these three windows we find spectral features diagnostic of the composition of the contents of Ontario Lacus. Our  $I/F$  (or radiance factor) spectra of the dark interior of Ontario Lacus (Fig. 2) show strong absorptions that are due mostly to methane gas in Titan’s atmosphere, as well as subtle variations within the windows at 2.0, 2.7 and 5.0  $\mu\text{m}$  as a result of photons scattered by Titan’s surface. To isolate the spectral differences between Ontario’s interior and its shoreline, and to remove atmospheric absorptions, we have constructed a ratio of representative spectra of the Ontario Lacus interior and a nearby area (with nearly identical viewing geometry) outside of the lake.

There are four apparent absorption features in the ratio spectrum (Fig. 2) that appear in only three of seven of Titan’s atmospheric windows, indicating that the detailed shapes of the atmospheric windows introduce no artefact absorptions. Thus, the remaining absorptions seen in the ratio are almost certainly associated with Ontario Lacus.

In order of increasing wavelength, the first of these bands is centred at 2.018  $\mu\text{m}$ , with a roughly gaussian profile. There is a second feature centred near 2.11  $\mu\text{m}$  that is quite weak and shows mostly as a depression in the long-wavelength wing of the 2.018- $\mu\text{m}$  band. The third band is centred near 2.79  $\mu\text{m}$  and is also roughly gaussian. The fourth feature is a very steep decline in reflectance near 4.8  $\mu\text{m}$ , which continues downwards out to 5.17  $\mu\text{m}$ . Within the region 4.8–5.17  $\mu\text{m}$  there also exist apparent narrow absorption features near 4.9 and 5.05  $\mu\text{m}$  whose significance is not clear.

An important indicator of whether a given absorption band in the Ontario Lacus spectrum pertains to material within the lake is whether the band is spatially correlated with the lake. In the 5- $\mu\text{m}$  image of Ontario Lacus (Fig. 1), the interior of the lake and the ‘beach’ are congruent to, but clearly have a much lower reflectivity than, the shoreline. Maps of the depths of the bands at 2.018 and 2.79  $\mu\text{m}$  have similar characteristics, although the weaker and noisier 2.79- $\mu\text{m}$  band shows much less correlation with the lake. We are therefore not convinced that the 2.79- $\mu\text{m}$  feature is real and do not discuss it further here.

The  $I/F$  at 5  $\mu\text{m}$  of the central, dark interior of Ontario Lacus approaches zero when extrapolated to zero airmass, indicating that almost all photons incident on the lake interior at this wavelength are absorbed (Fig. 3). In contrast to the finite reflectivity of a nearby area outside the lake (Fig. 3), the lake can only have zero reflectivity if its surface is smooth and free of scattering centres greater than about 5  $\mu\text{m}$  in size, the surface is viewed in non-specular geometry, and there are no slopes or facets allowing partial specular reflection along the line of sight. It is highly unlikely that any solid surface in the lake interior could adhere to such constraints, thus indicating that Ontario Lacus is filled with a quiescent liquid, free of particles larger than a few micrometres.

In view of the widespread evidence for precipitation on Titan<sup>8–10</sup>, an obvious question is whether liquid methane exists in Ontario Lacus. Unfortunately, because methane gas is so abundant in Titan’s atmosphere, and because the rotational–vibrational spectrum of liquid methane is nearly identical to that of methane gas (except for wavelength shifts that cannot be readily resolved in the VIMS data<sup>21</sup>), most features due to liquid methane would not be detectable in our spectra. Nevertheless, the steep decline in reflectance of Ontario Lacus within the 5- $\mu\text{m}$  window is consistent with the presence of other liquid alkanes such as ethane, propane and butane<sup>21–23</sup>.

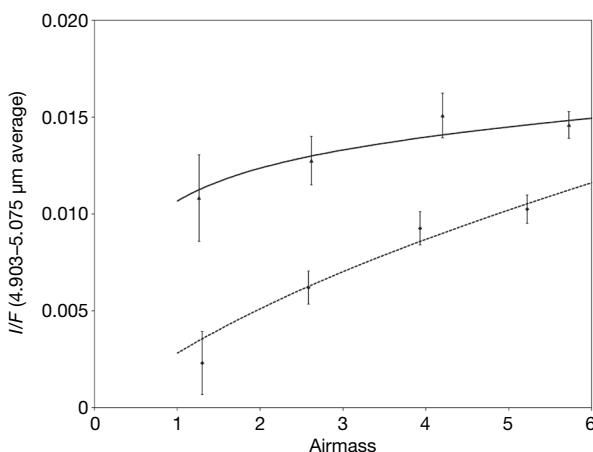


**Figure 3 | Plot of 5- $\mu\text{m}$  brightness against airmass for the lake interior and an adjacent region outside of Ontario Lacus.** The lake interior is denoted with diamonds (lower curve) and the adjacent area by triangles (upper curve). The lines show simple photometric models fitted to the points. Airmass here is the classical astronomical definition of atmospheric path length, commonly called  $\sec(z)$ , where  $z$  is the zenith angle referenced to the surface normal. Error bars are  $1\sigma$ .

An expected alkane on Titan is liquid ethane<sup>1</sup>. In addition to many bands that lie outside Titan's atmospheric windows, model spectra of liquid ethane show three absorption bands within the 2- $\mu\text{m}$  atmospheric window (Fig. 4). Two of the bands are blended into one apparent band at VIMS resolution and are centred at 2.018  $\mu\text{m}$  (ref. 22). The third band is centred at 2.11  $\mu\text{m}$ , very near the long-wavelength limit of the 2- $\mu\text{m}$  window, and is weaker than the 2.018- $\mu\text{m}$  band. The 2.018- $\mu\text{m}$  band complex in our model spectrum matches the central wavelength and shape of that in the Ontario Lacus data, but is slightly narrower. The 2.11- $\mu\text{m}$  band is very weak in the Ontario Lacus data in comparison with that in the model spectrum, showing only as a small depression in the long-wavelength wing of the 2.018- $\mu\text{m}$  band.

The apparent differences between the model spectrum and the lake spectrum are explained when atmospheric scattering and opacity are considered. This is demonstrated by using a model spectrum of ethane calculated for the 2- $\mu\text{m}$  atmospheric window (Fig. 5) that includes the effects of atmospheric scattering and opacity. The simulated bands are clearly shallower, and for the strongest band they are broader because the band wings increase as the band depth increases. There is also a substantial decrease in the depth of the weaker band near the long-wavelength edge of the window, making the band complex seem to be a single band with the long-wavelength wing suppressed. The Ontario Lacus ratio spectrum (Fig. 2) clearly shows that the long-wavelength wing of the 2.018- $\mu\text{m}$  band is suppressed precisely as expected if it were an ethane band. We therefore take this as identification of an additional ethane band at 2.11  $\mu\text{m}$ .

Another strong indicator of lake composition is the steep decline in reflectance beyond 4.8  $\mu\text{m}$ . This is characteristic of alkanes in general, and ethane, propane and butane in particular<sup>21–23</sup>. The spectrum of liquid ethane matches the short-wavelength portion of the deep 5- $\mu\text{m}$  absorption complex in Titan's spectrum (Fig. 4), and possible narrow features near 4.94 and 5.00  $\mu\text{m}$ . Although the reflectance of liquid ethane turns steeply upwards near the middle of the 5- $\mu\text{m}$  window, a small amount of propane, butane and higher-order alkanes could easily explain the continued decline in Titan's reflectance there<sup>23</sup>. We therefore consider this to be additional strong evidence for the presence of liquid ethane in Ontario Lacus, with a suggestion of other compounds such as propane and butane. Finally, although our data cannot unequivocally determine the presence or absence of liquid methane in Ontario Lacus, recent work on the seasonal evolution of hydrocarbon lakes on Titan shows that if liquid ethane exists in these lakes, in all probability so does liquid methane<sup>24</sup>.

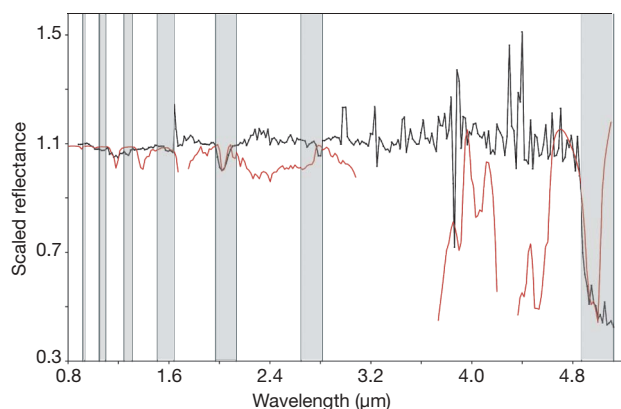


**Figure 4 | Ratio spectrum of Ontario's interior, with a model spectrum of liquid ethane superimposed.** The spectrum of liquid ethane is calculated for a path length of 300  $\mu\text{m}$  from tabulated absorption coefficients<sup>22</sup> and is convolved to the resolution and sampling interval of VIMS<sup>11</sup>. The black line shows the data, and the red line shows the model. The vertical grey bands denote the spectral channels within atmospheric windows through which VIMS can resolve surface detail.

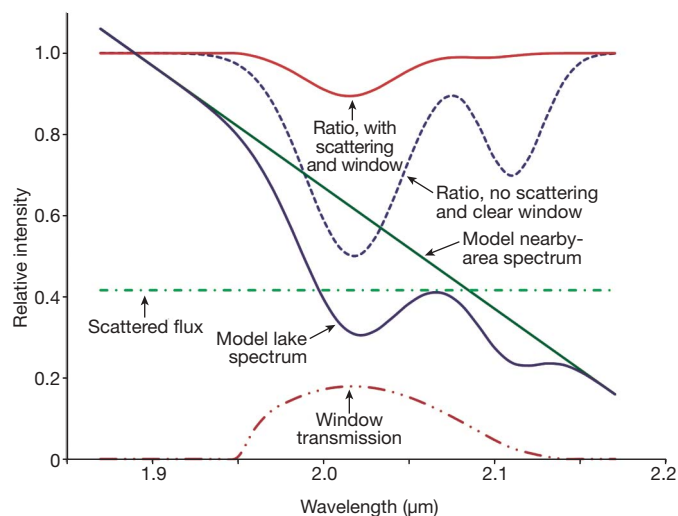


**Figure 5 | Model spectrum of liquid ethane simulating the effects of aerosol scattering and atmospheric opacity.** The model uses two gaussians of the same depth and width as those seen in the ethane spectrum to simulate the effects of scattering. The plot shows model spectra for areas inside and outside the lake, along with their ratio spectrum. Also shown is a contribution from scattered light, a model window-transmission function (constructed from two gaussians appropriate for the methane-gas absorption bands on either side of Titan's 2- $\mu\text{m}$  window), and the effect that scattering and the window opacity have on the resultant spectrum. In addition to photons scattered from the surface through an atmospheric window, a substantial number of photons are scattered by aerosols whose scattering function is roughly constant across the window (or at least having no spectral features that mimic those originating from the surface). Consequently, decreases in reflected intensity resulting from surface-spectral-absorption features cannot reduce the observed total intensity below the atmospheric scattering floor. The result is that observed spectral features introduced by photons scattered from surface materials are made shallower and broader by the contribution of the scattered photons from aerosols, but the centre wavelengths of the bands are left unchanged (again, so long as the scattering intensity does not vary much across the narrow window, which is true of Titan's 2- $\mu\text{m}$  window). As can be clearly seen, the simulated bands are shallower and, especially for the strongest band, broader because the band wings increase as the band depth increases. Also demonstrated is the substantial reduction in depth of the weaker band near the long-wavelength edge of the window, making the band complex look like a single band with the long-wavelength wing suppressed.

There are other possible materials in Ontario Lacus that we have considered but have rejected on the basis of the existing data from Titan. One candidate is water ice. It has a strong 2- $\mu\text{m}$  absorption and is very absorbing in the 5- $\mu\text{m}$  region, but its 2- $\mu\text{m}$  band is much too broad and centred at a slightly shorter wavelength<sup>25,26</sup>. Ammonia and ammonia hydrate both have bands near 2  $\mu\text{m}$ , but they are too narrow and also centred at a slightly shorter wavelength<sup>16,27</sup>. Carbon dioxide has a triplet centred near 2  $\mu\text{m}$ , but its components are too narrow and the complex is centred at a shorter wavelength<sup>16</sup>. Furthermore, all of the materials mentioned above are solid at Titan's temperatures and therefore none of them is likely to match the 5- $\mu\text{m}$  albedo of Ontario Lacus. There may be other simple compounds having bands in the 2- $\mu\text{m}$  region, but those discussed above are most plausible from a cosmochemical perspective<sup>28,29</sup>.

Received 28 February; accepted 19 May 2008.

1. Lunine, J. I., Stevenson, D. J. & Yung, Y. L. Ethane ocean on Titan. *Science* **222**, 1229–1230 (1983).
2. Lunine, J. I. Does Titan have an ocean—a review of current understanding of Titan's surface. *Rev. Geophys.* **31**, 133–149 (1993).
3. Lunine, J. I. Does Titan have oceans? *Am. Sci.* **82**, 134–143 (1994).
4. Dermott, S. F. & Sagan, C. Tidal effects of disconnected hydrocarbon seas on Titan. *Nature* **374**, 238–240 (1995).
5. Sagan, C. & Dermott, S. F. The tide in the seas of Titan. *Nature* **300**, 731–733 (1982).

6. Porco, C. C. *et al.* Imaging of Titan from the Cassini spacecraft. *Nature* **434**, 159–168 (2005).
7. Stofan, E. R. *et al.* The lakes of Titan. *Nature* **445**, 61–64 (2007).
8. Elachi, C. *et al.* Cassini radar views the surface of Titan. *Science* **308**, 970–974 (2005).
9. Elachi, C. *et al.* Titan radar mapper observations from Cassini's T-3 fly-by. *Nature* **441**, 709–713 (2006).
10. Tomasko, M. G. *et al.* Rain, winds and haze during the Huygens probe's descent to Titan's surface. *Nature* **438**, 765–778 (2005).
11. Brown, R. H. *et al.* The Cassini Visual and Infrared Mapping Spectrometer investigation. *Space Sci. Rev.* **115**, 111–168 (2004).
12. Griffith, C. A., Owen, T. & Wagnener, R. Titan's surface and troposphere, investigated with ground-based, near-infrared observations. *Icarus* **93**, 362–378 (1991).
13. Griffith, C. A., Owen, T., Geballe, T. R., Rayner, J. & Rannou, P. Evidence for the exposure of water ice on Titan's surface. *Science* **300**, 628–630 (2003).
14. Smith, B. A. *et al.* A new look at the Saturn System—the Voyager-2 images. *Science* **215**, 504–537 (1982).
15. Smith, B. A. *et al.* Encounter with Saturn—Voyager-1 imaging science results. *Science* **212**, 163–191 (1981).
16. Brown, R. H. & Cruikshank, D. P. Determination of the composition and state of icy surfaces in the outer solar system. *Annu. Rev. Earth Planet. Sci.* **25**, 243–277 (1997).
17. Lopes, R. M. C. *et al.* The lakes and seas of Titan. *Eos* **88**, 569–570 (2007).
18. Barnes, J. W. *et al.* A 5-micron-bright spot on Titan: evidence for surface diversity. *Science* **310**, 92–95 (2005).
19. Soderblom, L. A. *et al.* Correlations between Cassini VIMS spectra and RADAR SAR images: Implications for Titan's surface composition and the character of the Huygens Probe landing site. *Planet. Space Sci.* **55**, 2025–2036 (2008).
20. Barnes, J. W. *et al.* Global-scale surface spectral variations on Titan seen from Cassini/VIMS. *Icarus* **186**, 242–258 (2007).
21. Grundy, W. M., Schmitt, B. & Quirico, E. The temperature-dependent spectrum of methane ice I between 0.7 and 5  $\mu\text{m}$  and opportunities for near-infrared remote thermometry. *Icarus* **155**, 486–496 (2002).
22. Clark, R. N. *et al.* Detection of widespread aromatic and aliphatic hydrocarbons on Titan. *Icarus* (in the press).
23. Clark, R. N., Curchin, J. M., Hoefen, T. M. & Swayze, G. A. Reflectance spectroscopy of organic compounds. I: Alkanes. *J. Geophys. Res.* (submitted).
24. Mitri, G., Showman, A. P., Lunine, J. I. & Lorenz, R. D. Hydrocarbon lakes on Titan. *Icarus* **186**, 385–394 (2007).
25. Clark, R. N. & Lucey, P. G. Spectral properties of ice–particulate mixtures: Implications for remote sensing. I: Intimate mixtures. *J. Geophys. Res.* **89**, 6341–6348 (1984).
26. Clark, R. N. & McCord, T. B. The Galilean satellites: New near-infrared reflectance measurements (0.65–2.5  $\mu\text{m}$ ) and a 0.325–4.08  $\mu\text{m}$  summary. *Icarus* **43**, 323–339 (1980).
27. Brown, R. H., Cruikshank, D. P., Tokunaga, A. T. & Smith, R. G. Search for volatiles on icy satellites. I: Europa. *Icarus* **74**, 262–271 (1988).
28. Prinn, R. G. & Fegley, B. Kinetic inhibition of CO and N<sub>2</sub> reduction in circumplanetary nebulae—implications for satellite composition. *Astrophys. J.* **249**, 308–317 (1981).
29. Lewis, J. S. Chemistry of planets. *Annu. Rev. Phys. Chem.* **24**, 339–351 (1973).

**Author Information** Reprints and permissions information is available at [www.nature.com/reprints](http://www.nature.com/reprints). Correspondence and requests for materials should be addressed to R.H.B. ([rhb@lpl.arizona.edu](mailto:rhb@lpl.arizona.edu)).